

# Total-energy global optimizations using nonorthogonal localized orbitals

Jeongnim Kim

*Department of Physics, The Ohio State University, Columbus, Ohio 43210*

Francesco Mauri\* and Giulia Galli

*Institut Romand de Recherche Numérique en Physique des Matériaux (IRRMA), IN-Ecublens, 1015 Lausanne, Switzerland*

(Received 8 December 1994)

An energy functional for orbital-based  $O(N)$  calculations is proposed, which depends on a number of nonorthogonal, localized orbitals larger than the number of occupied states in the system, and on a parameter, the electronic chemical potential, determining the number of electrons. We show that the minimization of the functional with respect to overlapping localized orbitals can be performed so as to attain directly the ground-state energy, without being trapped at local minima. The present approach overcomes the multiple-minima problem present within the original formulation of orbital-based  $O(N)$  methods; it therefore makes it possible to perform  $O(N)$  calculations for an arbitrary system, without including any information about the system bonding properties in the construction of the input wave functions. Furthermore, while retaining the same computational cost as the original approach, our formulation allows one to improve the variational estimate of the ground-state energy, and the energy conservation during a molecular dynamics run. Several numerical examples for surfaces, bulk systems, and clusters are presented and discussed.

## I. INTRODUCTION

Most electronic structure calculations performed nowadays in condensed matter physics are based on a single-particle orbital formulation. Within this framework, the ground-state energy ( $E_0$ ) of a multiatomic system is obtained by solving a set of eigenvalue equations. Until recently, this was accomplished by searching directly the eigenstates of the single-particle Hamiltonian ( $\hat{H}$ ), which, in general, are extended states, e.g., Bloch states in a periodic system.<sup>1</sup>

In the last few years, methods for electronic structure (ES) calculations have been introduced, which are based on a Wannier-like representation of the electronic wave functions.<sup>2-8</sup> The main motivation for choosing such a representation was the search for methods for which the computational effort scales linearly with system size [ $O(N)$  methods]. Very recently, real space Wannier-like formulations were also used to describe the response of an insulator to an external electric field.<sup>9</sup> Within these approaches, a suitably defined total-energy functional ( $\mathbf{E}$ ) is minimized with respect to orbitals constrained to be localized in finite regions of real space, called localization regions. The minimization of the energy functional does not require the computation of either eigenvalues or eigenstates of  $\hat{H}$ .

In the absence of localization constraints, one can prove<sup>4</sup> that the absolute minimum of  $\mathbf{E}$  ( $\tilde{E}_0$ ) coincides with  $E_0$ . In the presence of localization constraints, a variational approximation to the electronic wave functions is introduced and therefore  $\tilde{E}_0$  lies above  $E_0$ . However, the difference between  $\tilde{E}_0$  and  $E_0$  can be reduced in a systematic way, by increasing the size of the localization regions. We note that localization constraints do not in-

troduce any approximation when the resulting localized orbitals can be obtained by a unitary transformation of the occupied eigenstates. Therefore, the use of localized orbitals is well justified for, e.g., periodic insulators, for which exponentially localized Wannier functions can be constructed by a unitary transformation of occupied Bloch states.<sup>10</sup>

The minimization of the functional  $\mathbf{E}$  with respect to *extended* states can be easily performed so as to lead directly to the ground-state energy  $E_0$ , without traps at local minima or metastable configurations.<sup>5</sup> On the contrary, the minimization of  $\mathbf{E}$  with respect to localized orbitals can lead to a variety of minima.<sup>5,7</sup> In order to attain the minimum representing the ground state, information about the bonding properties of the system has to be included in the input wave functions. This implies a knowledge of the system that may be available only in particular cases, and it constitutes the major drawback of the orbital-based  $O(N)$  method, which has otherwise been shown to be an effective framework for large-scale quantum simulations.<sup>11</sup>

In this paper, we propose a functional for orbital-based  $O(N)$  calculations, whose minimization with respect to localized orbitals leads directly to a physical approximation of the ground state, without traps at local minima. This overcomes the multiple-minima problem present within the original formulation<sup>4,5</sup> and makes it possible to perform  $O(N)$  calculations for an arbitrary system, with totally unknown bonding properties. The present formulation has also other advantages with respect to the original one. While retaining the same computational cost, it allows one to decrease the error in the variational estimate of  $E_0$ , for a given size of the localization regions, and to improve the energy conservation

during a molecular dynamics run.

The functional depends on a number of electronic orbitals ( $M$ ) larger than the number of occupied states ( $N/2$ ) of the  $N$ -electron system, and contains a parameter  $\eta$  determining the total charge. During the functional minimization,  $\eta$  is varied until the total charge of the system equals the total number of electrons; thus when convergence is achieved, i.e., the ground state is attained, the value of  $\eta$  coincides with that of the electronic chemical potential  $\mu$ . Once the ground state is obtained for a given ionic configuration, the corresponding wave functions and ionic positions can be used as a starting point for molecular dynamics simulations, which are then performed at fixed chemical potential. This is at variance with conventional ES calculations based on orbital formulations, where  $N$  is always fixed, e.g., by imposing orthonormality constraints. Similar to the present approach,  $O(N)$  calculations based on a density matrix formulation<sup>12</sup> are performed at fixed chemical potential. Consistently, the functional describing the total energy does not have multiple minima in the subspace of localized density matrices. However, whereas a density matrix approach presupposes the use of all the occupied and unoccupied states (i.e., a number of states equal to  $n_{\text{basis}}$ , where  $n_{\text{basis}}$  is the number of basis functions), in our formulation only a limited number of unoccupied states needs to be added to the set of occupied states, regardless of the basis set size. Therefore, the present formulation can be efficiently applied also in computations where the number of basis functions is much larger than the number of occupied states in the system (e.g., first-principles plane wave calculations).

The rest of the paper is organized as follows: In Sec. II, we present a generalization of the original formulation of orbital-based  $O(N)$  approaches; we first introduce an energy functional that depends on a number of orbitals larger than the number of occupied states, and we then discuss its properties and the role of the chemical potential. In Sec. III, we present the results of tight-binding calculations based on the generalized  $O(N)$  method, showing that the approach overcomes the multiple-minima problem, and allows one to improve on variational estimates of the ground-state properties and on the efficiency of molecular dynamics simulations. Conclusions are given in Sec. IV.

## II. ELECTRONIC STRUCTURE CALCULATIONS AT A GIVEN CHEMICAL POTENTIAL

### A. Definition of the functional

We consider the energy functional  $\mathbf{E}$  defined in Ref. 5, which depends on  $N/2$  occupied orbitals, for a  $N$ -electron system. We generalize  $\mathbf{E}$  so as to depend on an arbitrary number  $M$  of orbitals, which can be larger than the number of occupied states  $N/2$ . For simplicity, we consider a non-self-consistent Hamiltonian. The energy functional is written as

$$\mathbf{E}[\{\phi\}, \eta, M] = 2 \sum_{ij=1}^M Q_{ij} \langle \phi_j | \hat{H} - \eta | \phi_i \rangle + \eta N. \quad (1)$$

Here  $\{\phi\}$  is a set of  $M$  overlapping orbitals,  $\hat{H}$  is the single-particle Hamiltonian,  $\eta$  is a parameter, and  $\mathbf{Q}$  is a  $(M \times M)$  matrix:

$$\mathbf{Q} = 2\mathbf{I} - \mathbf{S}. \quad (2)$$

$\mathbf{S}$  is the overlap matrix:  $S_{ij} = \langle \phi_i | \phi_j \rangle$  and  $\mathbf{I}$  is the identity matrix. This definition of the  $\mathbf{Q}$  matrix corresponds to truncate the series expansion of the inverse of the overlap matrix to the first order ( $\mathcal{N} = 1$ , in the notation of Ref. 5). The charge density is defined as

$$\rho(\mathbf{r}) = 2 \sum_{ij=1}^M \langle \phi_j | \mathbf{r} \rangle \langle \mathbf{r} | \phi_i \rangle Q_{ij}. \quad (3)$$

For  $M = N/2$ , one recovers the original energy functional for  $O(N)$  calculations.

We note that the energy functional in Eq. (1) can be expressed in terms of a density matrix  $\hat{\sigma}[\{\phi\}]$ :

$$\mathbf{E}[\{\phi\}, \eta, M] = 2 \text{Tr}[(\hat{H} - \eta)\hat{\sigma}] + \eta N. \quad (4)$$

Here the trace is computed over the  $n_{\text{basis}}$  functions used for the expansion of the  $\{\phi\}$  and  $\hat{\sigma}[\{\phi\}] = \sum_{ij=1}^M |\phi_i\rangle Q_{ij} \langle \phi_j|$ .

Before discussing the use of the functional of Eq. (1) within a localized orbital formulation, it is useful to assess some of its general properties.

(i)  $\mathbf{E}[\{\phi\}, \eta, M]$  is invariant under unitary transformations of the type  $\phi'_i = \sum_{j=1}^M U_{ij} \phi_j$ , where  $\mathbf{U}$  is a  $(M \times M)$  unitary matrix.

(ii) Orbitals with vanishing norms do not give any contribution to the energy functional  $\mathbf{E}[\{\phi\}, \eta, M]$ . If the overlap matrix  $\mathbf{S}$  entering Eq. (1) has  $(M - M')$  eigenvalues equal to zero, then a unitary transformation  $\mathbf{U}$  exists, such that  $\{\phi'\}$  satisfies the condition

$$\langle \phi'_i | \phi'_i \rangle = 0 \quad \text{for } i = M' + 1, \dots, M. \quad (5)$$

Under this condition,

$$\mathbf{E}[\{\phi\}, \eta, M] = \mathbf{E}[\{\phi'\}, \eta, M']. \quad (6)$$

We note that if  $\mathbf{Q}$  is replaced by  $\mathbf{S}^{-1}$  in the definition of  $\mathbf{E}[\{\phi\}, \eta, M]$  [Eq. (1)], then orbitals with a vanishing norm give a nonzero contribution to the total energy, since for  $\langle \phi_i | \phi_i \rangle \rightarrow 0$  the eigenvalues of  $\mathbf{S}^{-1}$  go to infinity. Therefore, the functional  $\mathbf{E}[\{\phi\}, \eta, M]$ , with  $\mathbf{Q}$  replaced by  $\mathbf{S}^{-1}$ , does not satisfy property (ii).

(iii) The ground-state energy  $E_0$  is a stationary point of  $\mathbf{E}[\{\phi\}, \eta, M]$ . In order to prove this statement, we consider the following set of orbitals  $\{\phi^0\}$ :

$$\begin{aligned} |\phi_i^0\rangle &= |\chi_i\rangle \quad \text{for } i = 1, N/2 \\ |0\rangle & \quad \text{for } i = N/2 + 1, M, \end{aligned} \quad (7)$$

where  $|\chi_k\rangle$  are the  $n_{\text{basis}}$  eigenvectors of  $\hat{H}$  with eigenvalue  $\epsilon_k$ . Hereafter we assume that  $\langle \chi_k | \chi_k \rangle = 1$  and

$\epsilon_k \leq \epsilon_{k+1}$ . The set  $\{\phi^0\}$  fulfills Eq. (5); therefore,  $\mathbf{E}[\{\phi^0\}, \eta, M] = \mathbf{E}[\{\phi^0\}, \eta, N/2] = E_0$ . In addition, the set  $\{\phi^0\}$  is a stationary point of  $\mathbf{E}[\{\phi\}, \eta, M]$ , since  $\delta\mathbf{E}/\delta\phi_k|_{\{\phi^0\}} = 0$ , where

$$\frac{\delta\mathbf{E}}{\delta\phi_k} = 4 \sum_{j=1}^M [(\hat{H} - \eta)|\phi_j\rangle(Q_{jk}) - |\phi_j\rangle\langle\phi_j|(\hat{H} - \eta)|\phi_k\rangle]. \quad (8)$$

(iv) *The stationary point  $E_0$  is a minimum of  $\mathbf{E}[\{\phi\}, \eta, M]$  if  $\eta$  is equal to the electronic chemical potential  $\mu$ . We will only consider electrons at zero temperature; therefore, we choose  $\mu$  such that  $\epsilon_{N/2} < \mu < \epsilon_{N/2+1}$ . This property will be proved in the next section.*

### B. Role of the chemical potential

Before giving a proof of property (iv) stated in Sec. II A, we discuss a simple example, which is useful to illustrate the role played by  $\eta$  in the minimization of the energy functional  $\mathbf{E}$ . For this purpose, we evaluate the functional  $\mathbf{E}[\{\phi\}, \eta, M]$  for a set of  $M$  eigenstates of the Hamiltonian. In particular, we choose a set  $\{\phi\}$  such that  $|\phi_i\rangle = a_i|\chi_i\rangle$ , with arbitrary  $a_i$ . In this case, the energy functional becomes

$$\mathbf{E}[\{a\}, \eta, M] = 2 \sum_{i=1}^M (\epsilon_i - \eta)(2 - a_i^2)a_i^2 + \eta N. \quad (9)$$

As illustrated in Fig. 1, the function  $(\epsilon_i - \eta)(2 - a_i^2)a_i^2$  has a minimum at  $a_i = 0$  if  $\epsilon_i > \eta$ , and a minimum at  $a_i = 1$  if  $\epsilon_i < \eta$ . Thus, the functional  $\mathbf{E}[\{a\}, \eta, M]$  has a minimum for a set  $\{a^0\}$  such that  $a_i^0 = 1$  if  $\epsilon_i < \eta$ , and  $a_i^0 = 0$  if  $\epsilon_i > \eta$ . At the minimum, Eq. (9) becomes

$$E_{\min} = 2 \sum_{i=1}^{M'} \epsilon_i + \eta(N - 2M'), \quad (10)$$

where  $\epsilon_{M'} < \eta < \epsilon_{M'+1}$  and the total charge of the system is  $\rho_{\text{tot}} = 2 \sum_{i=1}^{M'} (2 - a_i^2)a_i^2 = 2M'$ . We can

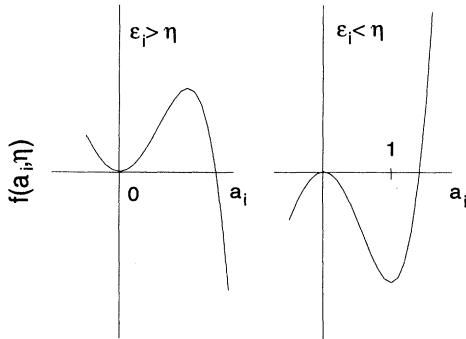


FIG. 1. Plot of the function  $f(a_i, \eta) = (\epsilon_i - \eta)a_i^2(2 - a_i^2)$  for a positive and a negative value of  $(\epsilon_i - \eta)$ .

now choose  $\eta$  so that  $\rho$  is equal to the actual number of electrons in the system. This is accomplished by setting  $\epsilon_{N/2} < \eta < \epsilon_{N/2+1}$ , i.e., by choosing  $\eta$  equal to the electronic chemical potential  $\mu$ . We then have  $\rho_{\text{tot}} = 2M' = N$  and  $E_{\min} = E_0$ .

In order to give a general proof of property (iv) (Sec. II A), we show that the Hessian matrix ( $h$ ) of the functional  $\mathbf{E}[\{\phi\}, \eta, M]$  at the ground state is positive definite, if  $\eta = \mu$ . The computation of the eigenvalues of  $h$  follows closely the procedure used in Ref. 5 to calculate the Hessian matrix of  $\mathbf{E}[\{\phi\}, \eta, N/2]$  at the ground state. Since the functional  $\mathbf{E}[\{\phi\}, \eta, M]$  is invariant under unitary rotations of the  $\{\phi\}$ , we can write a generic variation of the wave function with respect to the ground state as

$$\begin{aligned} |\phi_i^0\rangle &= |\chi_i\rangle + |\Delta_i\rangle \quad \text{for } i = 1, N/2 \\ |0\rangle + |\Delta_i\rangle & \quad \text{for } i = N/2 + 1, M, \end{aligned} \quad (11)$$

where

$$|\Delta_i\rangle = \sum_{l=1}^{n_{\text{basis}}} c_l^i |\chi_l\rangle. \quad (12)$$

By inserting Eq. (11) into Eq. (1), it is straightforward to show that the first-order term in the  $\{c\}$  coefficients vanishes for any value of the parameter  $\eta$ , consistently with property (iii) stated in Sec. II A. The remaining second-order term can be written as follows:

$$\begin{aligned} E^{(2)} &= \sum_{i=1}^{N/2} \sum_{m=N/2+1}^{n_{\text{basis}}} 2[\epsilon_m - \epsilon_i](c_m^i)^2 \\ &+ \sum_{ij=1}^{N/2} 8 \left[ \eta - \frac{(\epsilon_i + \epsilon_j)}{2} \right] \left[ \frac{1}{\sqrt{2}}(c_j^i + c_i^j) \right]^2 \\ &+ \sum_{i=N/2+1}^M \sum_{m=N/2+1}^{n_{\text{basis}}} 4[\epsilon_m - \eta](c_m^i)^2. \end{aligned} \quad (13)$$

The eigenvalues  $2[\epsilon_m - \epsilon_i]$  are independent of  $\eta$  and always positive, whereas the eigenvalues  $8[\eta - (\epsilon_i + \epsilon_j)/2]$  and  $4[\epsilon_m - \eta]$  are positive, if and only if  $\eta$  coincides with the chemical potential  $\mu$ . This proves property (iv) of Sec. II A.

## III. $O(N)$ CALCULATIONS WITH OVERLAPPING LOCALIZED ORBITALS

### A. Localization of orbitals and practical implementation

We now turn to the discussion of the functional defined in Sec. II A within a localized orbital formulation. The use of localized orbitals is a key feature to achieve linear system-size scaling<sup>5</sup> calculations. Orbitals are constrained to be localized in appropriate regions of space, called localization regions, i.e., they have nonzero components only inside a given localization region, whereas they are zero outside the localization region. The choice of the number of localization regions and of their centers

is arbitrary. In the calculations that will be discussed in the next sections, we chose a number of localization regions equal to the number of atoms, each centered at an atomic site ( $I$ ). We then associated an equal number of localized orbitals ( $n_s$ ) to a localization region, e.g., two and three localized orbitals for  $M = N/2$  and  $M = 3N/4$ , respectively. ( $M = Nn_s/n_{\text{val}}$ , where  $n_{\text{val}}$  is the number of valence electrons per atom.)

We will present electronic structure calculations and molecular dynamics simulations of various carbon systems, carried out within a tight-binding (TB) approach. We adopted the TB Hamiltonian proposed by Xu *et al.*,<sup>13,14</sup> which includes nonzero hopping terms only between the first-nearest neighbors. In a tight-binding picture, a localization region centered on the atomic site  $I$  can be identified with the set  $\{LR_I\}$  of atoms belonging to the localization region. Atoms are included in  $\{LR_I\}$ , if they belong to the  $N_h$  nearest neighbor of the center atom. Then, the localized orbital  $|\phi_i^L\rangle$ , whose center is the  $I$ th atom, is expressed as

$$|\phi_i^L\rangle = \sum_{J \in \{LR_I\}} \sum_l C_{Jl}^i |\alpha_{Jl}\rangle, \quad (14)$$

where  $|\alpha_{Jl}\rangle$ 's are the atomic basis functions of the atom  $J$  and the index  $l$  indicates the atomic components ( $s$ ,  $p_x$ ,  $p_y$ , or  $p_z$ ). In our computations, the generalized energy functional was minimized with respect to the localized orbitals  $\{\phi^L\}$  by performing a conjugate gradient (CG) procedure, both for structural optimizations and molecular dynamics simulations. For some calculations it was necessary to use a nonzero Hubbard-like term<sup>13</sup> to prevent unphysical charge transfers. In this case, the line minimization required in a CG procedure reduces to the minimization of a polynomial of eighth degree in the variation of the wave function along the conjugate direction. We performed an exact line minimization by evaluating the coefficients of the polynomial.

## B. The multiple-minima problem

As mentioned in the Introduction, the major drawback of the original formulation of orbital-based  $O(N)$  calculations is the so-called multiple-minima problem. Experience has shown that the minimization of  $\mathbf{E}[\{\phi\}, \eta, N/2]$  with respect to localized orbitals usually leads to a variety of minima,<sup>5,7</sup> and that the physical properties of the minimum reached during a functional minimization depend upon the choice for the input wave functions. If the input wave functions are constructed by taking advantage of bonding information about the ground state, then a minimum representing a physical approximation to the ground state may be reached, after an iterative minimization. On the contrary, if no information on the ground state is included in the localized orbitals from the start, the functional minimization usually leads to a local minimum, which is characterized by an unphysical charge density distribution.

This is illustrated for a particular case in Table I and Fig. 2, where we present the results of a series of TB

TABLE I. Cohesive energy  $E_c$  (eV) of a 256 carbon atom slab. The slab, consisting of 16 layers, represents bulk diamond terminated by a C(111)- $2 \times 1$  Pandey reconstructed surface on each side.  $E_c$  was obtained by performing localized orbital calculations with two and three states ( $n_s$ ) per atom (see text), and with three different inputs for the starting wave functions. Totally random input: The wave function expansion coefficients  $[C_{Jl}^i]$ , see Eq. (14)] on each site of a localization region (LR) are random numbers, and orbitals belonging to the same LR are orthonormalized at the beginning of the calculations. Atom by atom input: Each orbital has a nonzero  $C_{Jl}^i$  only on the atomic site to which it is associated, and for each atomic site this coefficient is chosen to be the same. Layer by layer input: Each orbital has a nonzero  $C_{Jl}^i$  only on the atomic site to which it is associated, and the value of this coefficient is chosen to be the same for each equivalent atom in a layer. In the case of atom by atom and layer by layer inputs, the initial wave functions are an orthonormal set. The calculations were performed with  $\eta=7.5$  eV and  $\eta=3.1$  eV for  $n_s=2$  and  $n_s=3$ , respectively, and with LR's extending up to second neighbors ( $N_h=2$ , amounting at most to 17 atoms per LR). The value for  $E_c$  obtained by direct diagonalization is 7.04 eV. (See also Fig. 1). The highest occupied and lowest unoccupied eigenvalues are 2.85 and 3.42 eV, respectively. In all calculations the Hubbard-like term was set at zero.

Wave function input	$E_c[n_s = 2]$	$E_c[n_s = 3]$
Totally random	6.837	6.978
Atom by atom	6.721	6.978
Layer by layer	6.930	6.978

calculations using localized orbitals, for a 256 carbon atom slab. The slab, consisting of 16 layers, represents bulk diamond terminated by a C(111)- $2 \times 1$  Pandey reconstructed surface on each side. We considered localization regions (LR's) extending up to second neighbors ( $N_h=2$ ). We performed conjugate gradient minimizations of the electronic structure using two localized orbitals per LR ( $n_s=2$ ), which correspond to the case  $M = N/2$  in Eq. (1), i.e., to the original formulation of  $O(N)$  calculations. These minimizations were carried out by starting from different wave function inputs. The only calculation that leads to a physical minimum was the one started with orbitals containing symmetry information about the system, as shown by comparing the results of Fig. 2(c) with those of direct diagonalization, reported in Fig. 3(b). The other calculations lead to unphysical minima: when starting with a totally random input [Fig. 2(a)], we found a local minimum with charged sites, located predominantly in the surface layers and in the middle of the slab. When starting from an atom by atom input [Fig. 2(b)], we obtained a local minimum corresponding to two differently charged surfaces, one positively and the other negatively charged.

The local minima problem present in the original  $O(N)$  formulation can be illustrated with a simple one-dimensional model.<sup>15</sup> We consider a linear chain with  $N_{\text{site}}$  sites and  $2N_{\text{site}}$  electrons in a uniform electric field of magnitude  $F$ , with Hamiltonian:

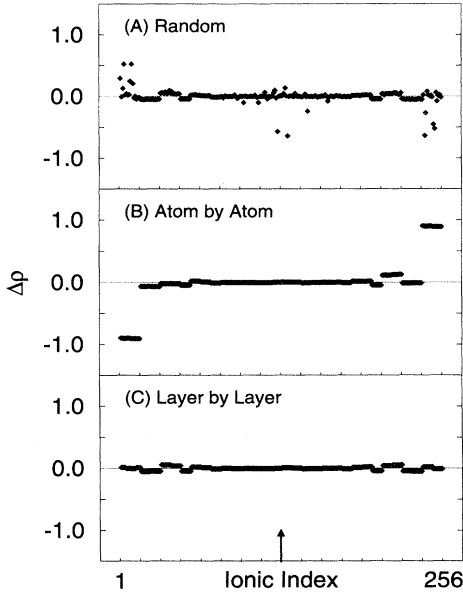


FIG. 2. Differential atomic charge ( $\Delta\rho$ ) on each atomic site of a 256 carbon atom slab. The slab, consisting of 16 layers, represents bulk diamond terminated by a C(111)- $2 \times 1$  Pandey reconstructed surface on each side. The ionic index indicates individual atomic sites belonging to the slab, which are ordered layer by layer, starting from the uppermost surface. The arrow indicates the slab center.  $\Delta\rho_K = \rho_K - \rho^0$ , where  $\rho_K = 2 \sum_{ij=1}^M \sum_l \langle \phi_i | \alpha_{Kl} \rangle Q_{ij} \langle \alpha_{Kl} | \phi_j \rangle$ ,  $\rho^0 = 4$ , and  $K$  is the atomic site. In (A), (B), (C) we show the results of calculations performed with two orbitals per atomic site, and with the three different wave function inputs listed in Table I, respectively.

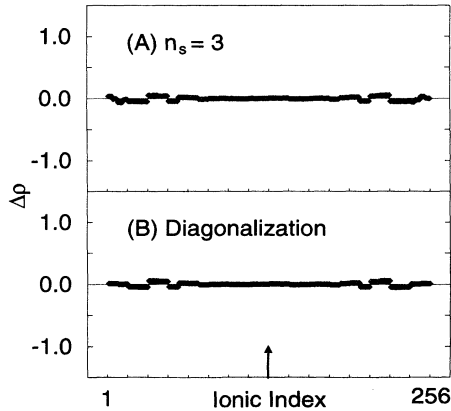


FIG. 3. Differential atomic charge ( $\Delta\rho$ ) on each atomic site for the same system as in Fig. 2. The ionic index is the same as in Fig. 2. In the upper panel we report the results of a calculation carried out with three orbitals ( $n_s$ ) per atomic site, and with a totally random input for the initial wave functions (see Table I). Contrary to the calculation started from a totally random input and performed with  $n_s=2$  [see Fig. 2(a)], the calculation with  $n_s=3$  gives a ground-state charge density very close to that obtained by direct diagonalization, shown in the lower panel.

$$\hat{H} = \sum_{K=1}^{N_{\text{site}}} [E_{\text{gap}} |e_K\rangle \langle e_K| - FK(|e_K\rangle \langle e_K| + |g_K\rangle \langle g_K|)]. \quad (15)$$

Here  $|e_K\rangle$  and  $|g_K\rangle$  are the highest and the lowest level of the isolated site  $K$ , respectively, and  $E_{\text{gap}}$  is the splitting between these two levels. Since the hopping terms between different sites are set at zero,  $|e_K\rangle$  and  $|g_K\rangle$  are also eigenfunctions of the linear chain Hamiltonian. We now study the ground state of the system as a function of the electric field  $F$ . If  $0 < F < E_{\text{gap}}/(N_{\text{site}} - 1)$ , the total energy of the system is minimized by the set of orbitals  $|\phi_i^0\rangle$  given by

$$|\phi_i^0\rangle = |g_i\rangle \quad \text{for } i = 1, N_{\text{site}}. \quad (16)$$

If  $E_{\text{gap}}/(N_{\text{site}} - 1) < F < E_{\text{gap}}/(N_{\text{site}} - 2)$ , the eigenvalue of  $|g_1\rangle$  is higher than that of  $|e_{N_{\text{site}}}\rangle$ , and therefore the total energy of the system is minimized by the following set of orbitals  $|\phi_i^0\rangle$ :

$$\begin{aligned} |\phi_i^0\rangle &= |g_{i+1}\rangle \quad \text{for } i = 1, N_{\text{site}} - 1 \\ &= |e_i\rangle \quad \text{for } i = N_{\text{site}}. \end{aligned} \quad (17)$$

In both cases, the total energy of the linear chain system can be obtained exactly within a localized orbital picture, by considering  $N_{\text{site}}$  LR's centered on atomic sites, which extend up to the first neighbors of a given site.

We first describe the total energy of the system with the functional  $\mathbf{E}[\{\phi\}, \eta, N/2]$ . Within this framework, the set  $|\phi_i^0\rangle$ , which minimizes  $\mathbf{E}[\{\phi\}, \eta, N/2]$  in the presence of a small field, i.e., when  $0 < F < E_{\text{gap}}/(N_{\text{site}} - 1)$ , is also a local minimum of  $\mathbf{E}[\{\phi\}, \eta, N/2]$  in the presence of a large field, i.e., when  $E_{\text{gap}}/(N_{\text{site}} - 1) < F < E_{\text{gap}}/(N_{\text{site}} - 2)$ . This can be easily seen from the second-order expansion ( $E^{(2)}$ ) of  $\mathbf{E}[\{\phi\}, \eta, N/2]$  around the set of orbitals defined in Eq. (16):

$$\begin{aligned} E^{(2)} &= \sum_{i=1}^{N_{\text{site}}} \sum_{m \in \{LR_i\}} 2[E_{\text{gap}} - F(m-i)](e_m^i)^2 \\ &+ \sum_{i=1}^{N_{\text{site}}} \sum_{j \in \{LR_i\}} 8 \left[ \eta + F \frac{i+j}{2} \right] \\ &\times \left[ \frac{1}{\sqrt{2}}(g_j^i + g_i^j) \right]^2, \end{aligned} \quad (18)$$

where  $g_K^i$  and  $e_K^i$  are the projection of the vector  $|\phi_i\rangle - |\phi_i^0\rangle$  on the state  $|g_K\rangle$  and  $|e_K\rangle$ , respectively. If the orbitals are extended, the difference  $(m-i)$  can be as large as  $(N_{\text{site}} - 1)$  and the eigenvalues  $[E_{\text{gap}} - F(m-i)]$  can be negative when  $E_{\text{gap}}/(N_{\text{site}} - 1) < F < E_{\text{gap}}/(N_{\text{site}} - 2)$ . However, if the orbitals are localized the difference  $(m-i)$  is smaller than  $(N_{\text{site}} - 1)$  and the eigenvalues  $[E_{\text{gap}} - F(m-i)]$  are always positive also for  $E_{\text{gap}}/(N_{\text{site}} - 1) < F < E_{\text{gap}}/(N_{\text{site}} - 2)$ .

We now turn to a description of the total energy of the linear chain system with the functional  $\mathbf{E}[\{\phi\}, \mu, M]$ , where  $M$  is larger than the number of occupied states  $N/2$ , e.g.,  $M = 2N_{\text{site}}$ . It is straightforward to show

that contrary to a description with  $\mathbf{E}[\{\phi\}, \eta, N/2]$ , when using  $\mathbf{E}[\{\phi\}, \mu, M]$  the set of orbitals of Eq. (16) is not a local minimum of the system in the presence of a large field. Indeed, according to Eq. (13), the second-order expansion  $E^{(2)}$  is now given by

$$\begin{aligned}
 E^{(2)} = & \sum_{i=1}^{N_{\text{site}}} \sum_{m \in \{LR_i\}} 2[E_{\text{gap}} - F(m-i)](e_m^i)^2 \\
 & + \sum_{i=1}^{N_{\text{site}}} \sum_{j \in \{LR_i\}} 8 \left[ \mu + F \frac{i+j}{2} \right] \\
 & \times \left[ \frac{1}{\sqrt{2}}(g_j^i + g_i^j) \right]^2 + \sum_{i=N_{\text{site}}+1}^{2N_{\text{site}}} \sum_{m \in \{LR_i\}} \\
 & \times 4[E_g - Fm - \mu](g_m^i)^2. \quad (19)
 \end{aligned}$$

Here the localized orbitals (LO's) with indices  $i$  and  $i + N_{\text{site}}$  are assigned to the localization region  $\{LR_i\}$ . Both within an extended and a localized orbital picture, the eigenvalue  $4[E_g - FN_{\text{site}} - \mu]$  is negative when  $E_{\text{gap}}/(N_{\text{site}} - 1) < F < E_{\text{gap}}/(N_{\text{site}} - 2)$ .

This simple model shows that the extremum properties of the functionals  $\mathbf{E}[\{\phi\}, \eta, N/2]$  and  $\mathbf{E}[\{\phi\}, \mu, M]$  are in general different, and in particular that local minima of  $\mathbf{E}[\{\phi\}, \eta, N/2]$  are not necessarily so for  $\mathbf{E}[\{\phi\}, \mu, M]$ . This suggests that the use of the functional  $\mathbf{E}[\{\phi\}, \mu, M]$  may overcome the multiple-minima problem encountered within a formulation based on  $\mathbf{E}[\{\phi\}, \eta, N/2]$ . This simple model suggests also the reason why the multiple-minima problem should be overcome: the minimization of  $\mathbf{E}[\{\phi\}, \mu, M]$  is performed by adjusting  $\mu$  until the total charge equals the total number of electrons in the system; this means that the appropriate filling of the orbitals is determined by the *global* variable  $\mu$ . This allows for long-range charge transfers in the minimization process, irrespective of the extent of the localization in the wave functions. Therefore, the presence of the *global* variable  $\mu$ , together with the augmented variational freedom of extra orbitals added to the definition of the functional, is expected to account for global changes taking place in the system.

### C. Overcoming the multiple-minima problem

We now present a series of numerical examples, showing that the minimization of the generalized functional  $\mathbf{E}[\{\phi\}, \eta, M]$  [Eq. (1)] with respect to localized orbitals can be performed without traps at local minima, as indicated by the simple model discussed in the previous section. We performed calculations for various carbon systems (bulk solids, surfaces, clusters, and liquids), by using again LR's extending up to second neighbors ( $N_h=2$ ). We considered three LO's per site ( $n_s=3$ ), i.e.,  $M = 3N/4$  in Eq. (1). In all cases, using  $n_s=3$  was sufficient to overcome the multiple-minima problem present in the original formulation. We note that the generalized functional, although it includes a number of localized orbitals larger than the number of occupied states,

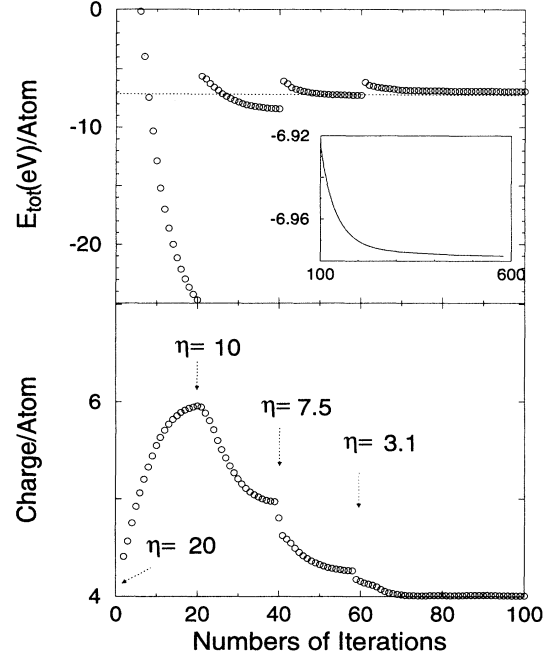


FIG. 4. Total energy  $E_{\text{tot}}$  (upper panel) and total charge (lower panel) per atom, as a function of the number of iterations, for an electronic minimization of the same system as in Figs. 1, 2, and Table I.  $E_{\text{tot}} = \mathbf{E}[\{\phi\}, \eta, M]$  (see text). The minimization was carried out with three states per atom ( $n_s=3$ ) and was started from a totally random input. The chemical potential ( $\eta$ ) was varied from 20 to 3.1 eV during the minimization. The final value of  $\eta$  was chosen so that the total charge eventually be equal to the number of electrons in the system. In the upper panel, the inset shows  $E_{\text{tot}}$  as a function of 500 iterations, converging to the value reported in Table I, and indicated as a dotted line.

still allows one to carry out electronic minimizations and molecular dynamics simulations with a computational effort scaling linearly with system size.

In Fig. 4, we show the energy and the charge per atom during a conjugate gradient minimization of  $\mathbf{E}[\{\phi\}, \eta, M]$ , for a 256 carbon atom slab, starting from a totally random input. The system is the same as the one studied in the previous section with  $n_s=2$ . The minimization was started with  $\eta = 20$  eV; the parameter was then decreased every 20 iterations, and finally set at 3.1 eV, which corresponds to the value of the chemical potential. As discussed in Sec. II B, for a given  $\eta$  the integral of the charge density converges to a value that corresponds to filling all the orbitals with energies smaller than  $\eta$ . For example, for  $\eta = 20$  eV the total charge per atom is equal to 6, i.e., all the  $3N/4$  orbitals are filled. Eventually, when  $\eta = \mu$  the total charge becomes equal to the number of electrons in the system. The way  $\eta$  is varied during a minimization is not unique; however, the final value of  $\eta$  must be always adjusted so as to obtain the correct charge in the system. It is seen in Table I that all the minimizations with  $n_s=3$  converge to the same value, irrespective of the input chosen for

TABLE II. Cohesive energy (eV) and length ( $\text{\AA}$ ) of the double and single bonds of  $C_{60}$ , as obtained from structural optimizations using localized (LO) and extended orbitals. In all calculations, the Hubbard-like term was set at zero. For comparison, cohesive energies obtained by direct diagonalization are given in parentheses. Computations with LO were performed by including two shells in a localization region ( $N_h=2$ , amounting to ten atoms per localization region), and by considering two and three orbitals ( $n_s$ ) per atom (see text).

Physical properties	Cohesive energy/atom	Double-bond distance	Single-bond distance
LO [ $N_h=2$ , $n_s=2$ ]	6.69 (6.89)	1.358–1.407	1.420–1.512
LO [ $N_h=2$ , $n_s=3$ ]	6.81 (6.91)	1.386–1.388	1.445–1.453
Extended orbitals	6.91	1.393	1.440

the wave function. This value corresponds to a physical minimum, as shown in Fig. 3 where we compare the charge density distribution with that obtained by direct diagonalization.

#### D. Improvement on variational estimates of the ground-state properties

The use of the generalized functional and LO's not only overcomes the problem of multiple minima, but it also improves the variational estimate of  $E_0$ , for a given size of the LR's. This is shown in Tables II and III, where we compare the results of calculations using the same LR's but different number of orbitals ( $n_s=2$  and 3), for various carbon systems. The improvement is particularly impressive in the case of  $C_{60}$ , where we also performed an optimization of the ionic structure. The error on the cohesive energy is decreased from 3 to 1.5% by increasing  $n_s$  from 2 to 3. Most importantly the optimized ionic structure obtained with  $n_s=3$  is in excellent agreement with that obtained with an extended orbital calculation. We note that localization constraints introduce a symmetry breaking in the system, i.e., LO's do not satisfy all the symmetry properties of the Hamiltonian eigenstates. In  $C_{60}$  the symmetry breaking is large

when using  $n_s=2$ ; the deviation of the double and single bond lengths with respect to their average values are 3.5 and 6.3%, respectively. On the contrary, in the optimized geometry obtained with  $n_s=3$ , the symmetry breaking is very small (0.1 and 0.5%, for the double and single bonds, respectively), compared to the icosahedral structure.

When using  $n_s=2$ , the ground-state LO's are nearly orthonormal,<sup>5</sup> whereas minimizations with  $n_s=3$  yield overlapping LO's. Indeed when using  $n_s=3$ , at the minimum the overlap matrix  $\mathbf{S}$  has  $2n_s$  eigenvalues close to 1 and  $n_s$  eigenvalues close to 0, and this condition can be satisfied with a nondiagonal  $\mathbf{S}$  matrix. We define a quantity measuring the orthogonality of the orbitals as  $\Delta^2 = [\sum_{ij=1}^M (\delta_{ij} - S_{ij})^2]/M$ . In the case of  $C_{60}$ ,  $\Delta^2$  is  $2.5 \times 10^{-3}$  and 0.17 for  $n_s=2$  and  $n_s=3$ , respectively. We also note that for various systems, the centers of the LO's  $\langle \mathbf{r}^L \rangle$ , defined as

$$\langle \mathbf{r}^L \rangle = \frac{\sum_K \sum_l \langle \phi^L | \alpha_{K,l} \rangle (\mathbf{r}_K) \langle \alpha_{K,l} | \phi^L \rangle}{\langle \phi^L | \phi^L \rangle}, \quad (20)$$

were always found to be located at distances shorter than one bond length from the center of their own LR's, when using  $n_s=3$ . In the case of  $n_s=2$ , we instead found cases, e.g., the  $C_{60}$  molecule, where some orbitals were centered

TABLE III. Cohesive energy  $E_c$  (eV) of different forms of solid carbon computed at a given bond length  $r_0$ . The calculations were performed with supercells containing 216, 128, and 100 atoms for diamond, two-dimensional (2D) graphite, and the linear chain, respectively. In calculations with localized orbitals we used two and three orbitals per atom ( $n_s$ , see text). The LR's included two shells of neighbors ( $N_h=2$ ), amounting to 17, 10, and 5 atoms per LR in the case of diamond, two-dimensional graphite, and the linear chain, respectively.

Crystal structure	Diamond ( $r_0 = 1.54 \text{ \AA}$ )	2D graphite ( $r_0 = 1.42 \text{ \AA}$ )	1D chain ( $r_0 = 1.25 \text{ \AA}$ )
$E_c$ [ $N_h=2$ , $n_s=2$ ]	7.16	7.09	5.62
$E_c$ [ $N_h=2$ , $n_s=3$ ]	7.19	7.12	5.67
$E_c$ [ $N_h=\infty$ ]	7.26	7.28	5.93

far from their atomic sites and close to the border of their LR's.

### E. Molecular dynamics simulations

In order to investigate the performances of the generalized functional [Eq. (1)] for molecular dynamics (MD) simulations, we carried out MD runs for liquid carbon at low density ( $2 \text{ gr cm}^{-3}$ ) and at 5000 K. We used a 64 atom cell with simple cubic periodic boundary conditions and only the  $\Gamma$  point to sample the Brillouin zone. We used a cutoff radius of  $2.45 \text{ \AA}$  for the hopping parameters entering the TB Hamiltonian and for the two-body repulsive potential<sup>13</sup> and  $U = 8 \text{ eV}$ . In the case of l-C it was necessary to add a Hubbard-like term to the Hamiltonian, in order to prevent unphysical charge transfers during the simulations. Equilibration of the system was performed in the canonical ensemble by using a Nosé thermostat.<sup>16</sup>

Within the original  $O(N)$  approach, MD runs for l-C were found to be particularly demanding from the computational point of view, since they required many iterations ( $N_{\text{iter}}$ ) per ionic move (e.g.,  $N_{\text{iter}}=300$  for  $\Delta t=30$  a.u.), in order to minimize the energy functional.<sup>5</sup> Most importantly, during the simulation the system could be trapped at a local minimum, evolve adiabatically from that minimum for some time, and suddenly jump to another minimum lower in energy. This shows up as a spike in the constant of motion of the system ( $E_{\text{const}}$ ), as can be seen in line (c) of Fig. 5, which displays  $E_{\text{const}}$  for a run performed with  $n_s=2$ . Because of local minima, a perfect conservation of energy could never be achieved with  $n_s=2$ , even by increasing  $N_{\text{iter}}$  to a very large number.

When MD runs are performed with  $n_s=3$ , the problem of local minima is overcome; furthermore a significant improvement in the conservation of energy can be achieved at the same computational cost as simulations with  $n_s=2$ . This is seen in Fig. 5 by comparing lines (b) and (c). When the generalized functional is used, the accuracy of the energy conservation during a MD run is related only to the convergence of the electronic minimization scheme: a good conservation of energy can be obtained just by increasing  $N_{\text{iter}}$ . This is shown by line (a) in Fig. 5. We note that the behavior of  $E_{\text{const}}$  observed for all the simulations was not affected by the presence of the thermostat. This was checked by repeating all MD runs with three different masses ( $Q_s$ ) for the Nosé thermostat ( $Q_s=1,4,100$  in the same units). The structural properties of l-C computed from the MD runs with  $n_s=3$  showed a very good agreement with those previously obtained with  $n_s=2$ .

## IV. CONCLUSIONS

We have presented a generalization of orbital-based  $O(N)$  approaches, which relies upon a functional, depending on a number of localized states larger than the number of occupied states, and on a parameter that determines the total number of electrons in the system. We have shown that the minimization of this functional with respect to localized orbitals can be carried out without traps at local minima, irrespective of the input chosen

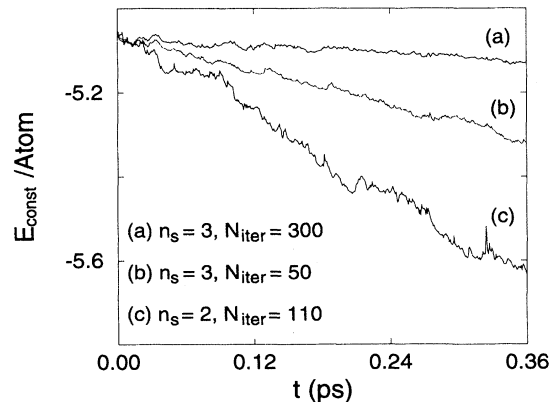


FIG. 5. Energy per atom ( $E_{\text{const}}$ ) as a function of the simulation time ( $t$ ) for constant temperature ( $T$ ) molecular dynamics (MD) simulations of liquid C.  $E_{\text{const}} = E_{\text{kin}} + \mathbf{E}[\{\phi\}, \eta, M] + E_{\text{thrms}}$ , where  $E_{\text{kin}}$  is the ionic kinetic energy,  $\mathbf{E}[\{\phi\}, \eta, M]$  is the ground-state value of the electronic energy functional (see text), and  $E_{\text{thrms}}$  is the sum of the potential and kinetic energies associated to the Nosé thermostat. The LR's extend up to second neighbors. ( $N_h=2$ , amounting on average to 18 atoms per LR.) (a) and (b) correspond to MD runs with three states per atom ( $n_s=3$ ), whereas (c) corresponds to a simulation with  $n_s=2$ . The time step used in the three MD runs was 30 a.u. (0.73 fs). At each step, the electronic structure was minimized by a conjugate gradient procedure with a fixed number of iterations ( $N_{\text{iter}}$ ). The simulations represented by lines (b) and (c) require the same computational cost.

for the wave functions. In this way, the multiple-minima problem present in the original formulation is overcome, and  $O(N)$  computations can be performed for an arbitrary system, without knowing any bonding properties of the system for the calculation input. We have also presented a series of tight-binding calculations for various carbon systems, showing that the generalized  $O(N)$  approach allows one to decrease the error in the variational estimate of the ground-state properties, and to improve energy conservation, i.e., efficiency, during a molecular dynamics run. This can be accomplished at the same computational cost as within the original formulation. At variance from  $O(N)$  density matrix approaches, our formulation requires that only a limited number of unoccupied states be included in the energy functional, regardless of the basis set size. Therefore, the present formulation can be efficiently applied also in computations where the number of basis functions is much larger than the number of occupied states in the system (e.g., first-principles plane wave calculations).

## ACKNOWLEDGMENTS

It is a pleasure to thank A. Canning, A. Dal Corso, M. Steiner, and J. W. Wilkins for useful discussions and a critical reading of the manuscript. This work was partly supported by DOE (J. K.) and by the Swiss National Science Foundation under Grant No. 20-39528.93 (G. G. and F. M.).



\* Present address: Department of Physics, University of California at Berkeley, Berkeley, CA 94720.

- <sup>1</sup> For a review, see, e.g., G. Galli and A. Pasquarello, in *Computer Simulation in Chemical Physics*, edited by M. P. Allen and D. J. Tildesley (Kluwer, Dordrecht, 1993), p. 261; M. C. Payne, M. P. Teter, D. C. Allan, T. A. Arias, and J. D. Joannopoulos, *Rev. Mod. Phys.* **64**, 1045 (1993).
- <sup>2</sup> G. Galli and M. Parrinello, *Phys. Rev. Lett.* **69**, 3547 (1992).
- <sup>3</sup> W.-L. Wang and M. Teter, *Phys. Rev. B* **46**, 12 798 (1992).
- <sup>4</sup> F. Mauri, G. Galli, and R. Car, *Phys. Rev. B* **47**, 9973 (1993).
- <sup>5</sup> F. Mauri and G. Galli, *Phys. Rev. B* **50**, 4316 (1994).
- <sup>6</sup> P. Ordejón, D. Drabold, M. Grunbach, and R. Martin, *Phys. Rev. B* **48**, 14 646 (1993).
- <sup>7</sup> P. Ordejón, D. Drabold, M. Grunbach, and R. Martin, *Phys. Rev. B* **51**, 1456 (1995).
- <sup>8</sup> W. Kohn, *Chem. Phys. Lett.* **208**, 167 (1993).
- <sup>9</sup> R. W. Nunes and D. Vanderbilt, *Phys. Rev. Lett.* **73**, 712 (1994); A. Dal Corso and F. Mauri, *Phys. Rev. B* **50**, 5756 (1994).
- <sup>10</sup> W. Kohn, *Phys. Rev.* **115**, 809 (1959); *Phys. Rev. B* **7**, 4388 (1973).
- <sup>11</sup> G. Galli and F. Mauri, *Phys. Rev. Lett.* (to be published).
- <sup>12</sup> X.-P. Li, R. Nunes, and D. Vanderbilt, *Phys. Rev. B* **47**, 10 891 (1993); M. S. Daw, *ibid.* **47**, 10 895 (1993).
- <sup>13</sup> C. Xu, C. Wang, C. Chan, and K. Ho, *J. Phys. Condens. Matter* **4**, 6047 (1992).
- <sup>14</sup> We used a cutoff radius of 2.30 Å for the hopping parameters of  $\hat{H}$  and for the two-body repulsive potential, and  $U=0$  eV for the Hubbard-like term (see Ref. 13).
- <sup>15</sup> A similar model was used by D. Vanderbilt to show numerically the presence of local minima in the functional  $\mathbf{E}[\{\phi^0\}, \eta, N/2]$  (private communication).
- <sup>16</sup> S. Nosé, *Mol. Phys.* **52**, 255 (1984); W. Hoover, *Phys. Rev. A* **31**, 1695 (1985).